Journal of Cardiovascular Disease Research

ISSN:0975 -3583,0976-2833 VOL 12, ISSUE 09, 2021

Investigating Cumulative Fission Yields in 238UInduced by 14.7 MeV Neutrons

1SATISH KUMAR K,2 SANDHYA LAKKARSU
12Assistant Professor
DEPT of H&S
Vaagdevi College of Engineering, Warangal, TS, India

ABSTRACT:

This study presents the results of cumulative fission yield measurements performed on uranium-238 (238U^{238}\text{U}238U) using 14.7 MeV neutrons. Cumulative fission yield refers to the total amount of fission products produced after a neutron-induced fission event, which is critical for understanding the behavior of nuclear materials in both research and practical applications, such as nuclear power generation and radioactive waste management.

Using a specialized experimental setup, 238U^{238}\text{U}238U samples were subjected to controlled neutron bombardment at the specified energy level. The fission products were then analyzed to quantify the cumulative yields. The methodology involved the detection and identification of fission products through advanced spectroscopy techniques, which allowed for high-precision measurements.

Preliminary results indicate significant variations in the cumulative fission yields of various isotopes, highlighting the influence of neutron energy on the fission process. Additionally, the data obtained contribute to a more comprehensive understanding of the fission pathways in 238U^{238}\text{U}238U and offer valuable insights for improving models of neutron-induced fission reactions.

Keywords: activation process, DT neutron source, fission yields, 238U

1. INTRODUCTION

Uranium-238 (238U^{238}\text{U}238U) is the most abundant isotope of uranium, constituting over 99% of naturally occurring uranium. Its significance in nuclear science and technology arises from its role as a fertile material in nuclear reactors and its potential for transmutation into fissile isotopes, such as 239Pu^{239}\text{Pu}239Pu through neutron capture. Understanding the fission properties of 238U^{238}\text{U}238U, particularly its cumulative fission yields, is crucial for advancing nuclear energy applications and improving the management of radioactive waste.

Cumulative fission yield measurements are essential for characterizing the distribution of fission products generated during nuclear fission processes. These measurements provide insights into the underlying fission mechanisms, including the dynamics of neutron interactions and the subsequent decay pathways of fission products. The yields can vary significantly depending on the energy of the incident neutrons, the composition of the target material, and the specific fission pathways involved.

This study focuses on cumulative fission yield measurements of 238U^{238}\text{U}238U induced by 14.7 MeV neutrons. The choice of this neutron energy is significant, as it is commonly employed in various nuclear applications, including neutron activation analysis and fusion research. By investigating the fission yield at this energy level, we aim to contribute to the existing body of knowledge on neutron-induced fission processes and enhance the predictive capabilities of fission yield models.

The experimental approach involves exposing 238U^{238}\text{U}238U samples to a controlled flux of 14.7 MeV neutrons and subsequently analyzing the resulting fission products using advanced detection techniques. These techniques facilitate high-precision measurements, allowing for the identification and quantification of individual isotopes produced during the fission process.

In the following sections, we will discuss the experimental methodology, present the results of our measurements, and analyze the implications of our findings in the context of

ISSN:0975 -3583,0976-2833 VOL 12, ISSUE 09, 2021

nuclear physics and engineering. This research not only enhances our understanding of fission dynamics in 238U^{238}\text{U}238U but also serves as a valuable resource for future studies on fission yield characteristics across a range of nuclear materials.

II. EXPERIMENT DETAILS

A. Target preparation and irradiation

Before using the D-T neutron to induce 238U fission, two natural triuranium octaoxide (U3O8) powder samples (99.9% purity) were made into round disks of 20 mm diameter with thicknesses 1.1 mm (U-1 sample) and 1.0 mm (U-2 sample). Each sample was placed between a Nb foil (diameter: 20 mm, thickness: 0.01 mm, purity: 99.999%) and Zr foil (diameter: 20 mm, thickness: 0.01 mm, purity: 99.99%). A 93Nb(n, 2n)92mNb reaction was used to monitor neutron flux, and the decay data are summarized in Table 1. Simultaneously, the sandwich sample was covered with a Cd box for preventing scattering of thermal neutrons. During the irradiation, three sandwich samples were placed approximately 6.0 cm away from the T-Ti target relative to the deuteron beam's incident direction at 35° (see Fig. 1).

The irradiation was carried out on the K-400 neutron generator (the yield is approximately 3 × 1010 n/4πs) at Institute of Nuclear Physics and Chemistry, China Academy of Engineering Physics. In order to obtain a mass distribution of fission products as completely as possible, the fission product nuclei with different lifetimes should be irradiated in batches. The irradiation time of the U-1 sample was 60 min for the measurement of fission product nuclei with a lifetime of a few hours. To measure longer-lived fission product nuclei, the U-2 sample was irradiated for 17 h. The T(d, n)4He reaction with a deuteron beam (250 keV, 180 μA) produced 14 MeV neutrons. The energies of neutrons were measured using the cross-section ratio of 93Nb(n, 2n)92mNb to 9089

Zr(n, 2n) Zr reaction and compared with results of mean neutron energy calculation [20, 21], which were 14.7 ± 0.2 at 35°. The Au-Si detector relative to the deu4 teron beam at 135° monitored the accompanying He particle to measure the neutron yield and neutron flux per 10 s, which would give a correction for neutron fluctuation.

B. HPGe detector efficiency calibration

Before irradiation, a series of standard point sources

Table 1. The decay data of monitor reaction and fission products.

Activation products	Half-life of product $T_{1/2}$	Gamma-ray energy/keV	Gamma-ray intensity I^{γ} (%)
$^{90}Zr(n,2n)^{89}Zr$	78.41±0.12 h	909.15	99.04±0.03
$^{93}Nb(n,2n)^{92m}Nb$	10.15±0.02 d	934.44	99.15±0.04
^{91}Sr	9.65±0.06 h	1024.3	33.5±1.1
^{92}Sr	2.611±0.017 h	1383.93	90±6
^{93}Y	10.18±0.08 h	266.9	7.3±1.1
^{96}Zr	64.032±0.006 d	756.73	54.38±0.22
^{97}Zr	16.749±0.008 h	743.36	93.09±0.16
^{99}Mo	65.924±0.006 h	739.5	12.20±0.16
^{103}Ru	39.247±0.013 d	610.3	5.76±0.06
^{103}Ru	4.44±0.02 h	724.4	47.3±0.5
^{127}Sb	3.85±0.05 d	685.7	36.8±2.0
^{128}Sn	59.07±0.14 min	482.3	59±7
^{131}I	8.0252±0.0006 d	364.49	81.5±0.8
^{137}Te	3.204±0.013 d	228.1	88±3
^{131}I	20.83±0.08 h	529.87	87.0±2.3
^{134}Te	40.8±0.8 min	767.2	29.5±1.4
^{135}I	6.58±0.03 h	1260.41	28.7±0.9
^{140}Ba	12.7527±0.0023 d	537.26	24.39±0.22
^{140}La	91.1±0.5 min	641.3	47.4±0.5
^{143}Ce	33.039±0.006 h	293.27	42.8±0.4
^{147}Nd	10.98±0.01 d	531.01	13.4±0.3
^{149}Nd	1.728±0.001 h	270.17	10.7±0.5

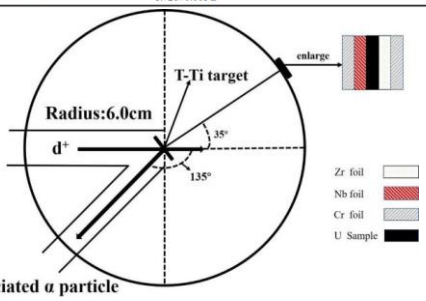

Fig. 1. (color online) Schematic diagram of experimental geometry [22].

(22Na, 60Co, 133Ba,137Cs, 152Eu) of known activity were used to determine the absolute full energy peak effi- ciency of a lead-shielded high purity germanium detector (HPGe type: GEM60P, produced by ORTEC) with a rel- ative efficiency of 68% and an energy resolution of 1.82 keV at 1.33 MeV for 60Co. The detection efficiencies (εp) for the point source placed at distances of 4.5 cm and 9 cm from the detector were both determined by Eq. (1) [23]:

$$\epsilon_p = \frac{C}{A_0 e^{-\lambda t} \Delta t I_\gamma}, \qquad (1)$$

ISSN:0975 -3583,0976-2833 VOL 12, ISSUE 09, 2021

where C is the number of counts during the counting
time, A0 is the source activity at the time of manufacture, t is the time elapsed from the date of manufacture to the start time of counting, λ is the decay constant, and Iγ is the decay γ intensity.

In order to obtain the detector efficiencies at the char- acteristic γ energies of the fission nuclides, the depend- ence of the full energy peak efficiency versus the energy was described by an exponential function, as expressed in Eq. (2) [24]. The fitting parameter values are given in Fig. 2.

$$\epsilon_p = \frac{C}{A_0 e^{-\lambda t} \Delta t I_\gamma}, \qquad (1)$$

C.Measurement of γ-ray activity

After completion of the neutron irradiation and suffi- cient cooling, the two U samples and Nb samples were transferred to a pre-calibrated HPGe detector. The data acquisition was carried out using the program MAES- TRO. By extending the sample cooling time or increas- ing the distance between the sample and the detector, it is possible to significantly lessen the impact of dead time on the statistical count of high purity germanium detectors with high count rate samples. Therefore, the U-1 sample was measured at a distance of 9 cm from the detector

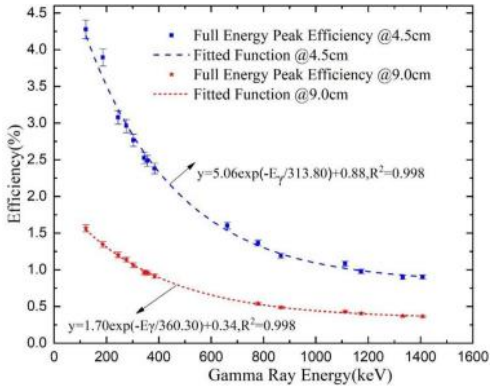

Fig. 2. (color online) The fitted efficiency curve and meas-ured efficiency data.

after 76.53 min of cooling. In order to improve the accur- acy of short-lived nuclide counting, it is necessary to per- form dead time correction. The U-1 and U-2 samples were measured after 22.08 h and 20.59 days, respectively, at a distance of 4.5 cm from the detector, and the dead time was negligible.

As shown in Fig. 3, hundreds of different energy characteristic gamma rays were measured by a high-purity germanium detector. In order to identify whether each gamma ray is emitted by the radionuclide of interest, the decay curve analysis method is adopted to identify the radionuclide by measuring the half-life of the radionuclide, which has been discussed in our previous article [25]. We take the 743.36 keV γ-ray produced by the ^{97}Zr nucleus as an example, which may be affected by the very close energy γ-ray (743.66 keV, 16.1%) from ^{130}Sn ($T_{1/2}$=3.72

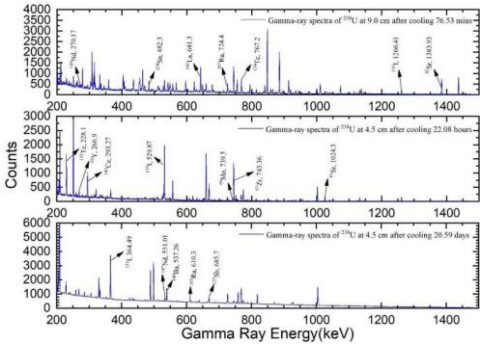

Fig. 3. (color online) The background subtracted gamma spectrum of different fission products of the 238U sample. (a) U-1 sample at 9 cm with 1369 s lifetime; (b) U-1 sample at 4.5 cm with 3600 s lifetime; (c) U-2 sample at 4.5 cm with 10800 s lifetime. min) and by the 743.3 keV (100%) gamma ray from 128Sb (T =9.05 h). Because the half-life of 130Sn is short and the cumulative fission yield of 128Sb is one order of mag- nitude lower than that of 97Zr, there is a good agreement between the half-life obtained by periodical measure- ment as shown in Fig. 4 (17.04 h) and the recommended half-life (16.75 h) of 97Zr. When the relative deviation between the experimental value and recommended value is less than 5%, it will be selected for the final fission yield calculation [18]. By using this method, twenty char- acteristic gamma rays (as shown in Fig. 4) were selected to calculate the fission yield. The decay characteristics of the product radioisotopes are summarized in Table 1.

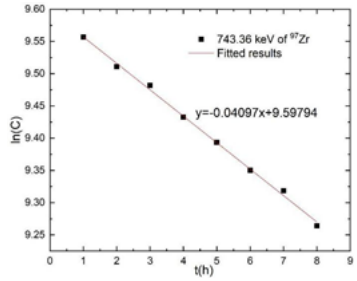

Fig. 4. (color online) Relationship between measurement time of 97Zr and logarithm of characteristic peak counts.

ISSN:0975 -3583,0976-2833 VOL 12, ISSUE 09, 2021

III. DATA & ANALYSIS

A. Calculation of fission product yields

The number of detected γ-rays corresponding to the activity of fission products was obtained from their total peak areas by subtracting the linear Compton background. The number of detected γ-rays under the photopeak of an individual fission product is related to their cumulative yields as follows [4]:

$$Y = \frac{C\lambda f_{all}}{\Phi \sigma_f N_u \epsilon I_\gamma (1-e^{-\lambda t_1}) e^{-\lambda t_2} (1-e^{-\lambda t_3})}, \quad (3)$$

where
is the net area of the photoelectric peak of the measured characteristic gamma rays; λ is the dec ay constant of the fission product;
is the fission cross section of 238U at the neutron energy used;
is the number of 238U in the target;
is the detection efficiency of the high purity germanium detector system; , , and denote the where C is the net area of the photoelectric peak of the measured characteristic gamma rays; λ is the decay constant of the fission product;σf is the fission cross section of 238U at the neutron energy used;Nu is the number of
238 U in the target;ϵ is the detection efficiency of the high purity germanium detector system;t1,t2, and t3denote the irradiation time, cooling time, and real measurement time, respectively; fall is the correction factor; and Φ is the neutron flux, which can be obtained from the monitor foil Nb as shown in Eq. (4):

$$\Phi = \frac{C' \lambda' f'_{all}}{N' \sigma' \epsilon' I'_\gamma (1-e^{-\lambda' t_1}) e^{-\lambda' t_2} (1-e^{-\lambda' t_3})}, \quad (4)$$

where C′ is the net area of the photoelectric peak of the measured characteristic gamma rays of 92mNb; λ′ is the 92m decay constant of Nb; σ′ is the cross section of the 93 92m Nb(n, 2n) Nb reaction at the neutron energy used; N′ is the number of 93Nb in the monitor target; ϵ′ is the detection efficiency of the 934.44 keV γ ray in the high purity germanium detector; t1, t2′ , and t3′ denote the irradiation time, cooling time, and real measurement time of the Nb sample, respectively; and fall′ is the correction factor.

B. Correction factor calculation

In the nuclear reaction data measurement by the activation method there are some corrections such as photon attenuation, neutron flux fluctuation, cascade summing correction, scattered neutron correction, dead time correction, and isotopic impurities. The main correction factor in Eq. (3) and main uncertainty sources are introduced in this section.

1. Photon attenuation Gamma rays are emitted throughout the target volume and experience self-absorption before reaching the detector, which causes the count reduction. Before determining the yield, the self-absorption effect must be corrected to establish the absolute activity of any fission products in
the target. According to the attenuation law of γ-rays in matter, the correction factor can be calculated as expressed in Eq. (5):

$$F = \frac{1-e^{-\mu(E)x}}{\mu(E)x}, \quad (5)$$

where μ(E) is the energy-dependent mass attenuation coefficient (cm2·g−1), and x is the product of the material density and “effective” thickness of the sample (g·cm−2). Values for μ(E) for uranium metal were obtained from the National Institute of Standards & Measurements: XCOM database [26]. According to the ratio of U and O, the total mass attenuation coefficient of different gamma ray energies of U and O materials could be obtained by interpolation.

2. Beam fluctuation correction

The accelerator neutron source cannot be completely stable during long time irradiation; hence, the neutron injection rate fluctuates to a certain extent and needs to be corrected. The correction factor K is calculated using Eq.(6):

$$K = \left[\sum_i^L \Phi_i (1-e^{-\lambda \Delta t_i}) e^{-\lambda T_i}\right] / \Phi S, \quad (6)$$

where L is number of time intervals into which the irradiation time is divided, Δti is the duration of the ith time interval, Ti is time interval from the end of the ith interval to the end of irradiation, and Φi is neutron flux averaged over the sample during Δti.

3. Cascade summing correction

For the fission product yield measurement, cascade summing correction is non-negligible.

ISSN:0975 -3583,0976-2833 VOL 12, ISSUE 09, 2021

Because of the time consistency, it is possible that one or more of the γrays are simultaneously recorded by the HPGe detector, resulting in the count addition or loss of the characteristic gamma-ray peak. This effect is particularly position dependent for each fission product [18]. The correction factor of cascade summing can be simply written as Eq. (7). A detailed calculation of cascade coincidence correction coefficient can be found in Ref. [27]:

$$C = S/S', \qquad (7)$$

where S is the full-energy peak intensity of the characteristic γ ray if there is no cascade coincidence effect, andS′ is the actual observed full-energy peak intensity of the characteristic γ ray.

The correction factors of photon attenuation, neutron flux fluctuation, and cascade summing correction as well as the total correction factor are summarized in Table 2.

4. Uncertainties

The main uncertainties in the presented measurements are summarized in Table 3, which include photoelectric peak area (0.1%–5%), gamma ray emission probability (0.1% –15%), photoelectric peak detection efficiency (2.0%–3.0%), half-life (0.01%–0.93%), and coincidence summing (3%). The cross-section uncertainty (0.6%) of the 238U(n, f) reaction was obtained by an interpolation method from literature [28]. The total uncertainty (4.62% –16.45%) in the present work is the quadratic summation of the given uncertainties.

IV. RESULTS AND DISCUSSION

Table 2. Values of correction factors.

Fission products	Photon attenuation	Beam fluctuation	Coincidence summing	Total correction factor
^{91}Sr	1.0063	0.9991	1.0229	1.0284
^{92}Sr	1.0049	0.9961	1.0034	1.0044
^{93}Y	1.0586	0.9992	1.0064	1.0645
^{95}Zr	1.0089	1.0001	0.9848	0.9937
^{97}Zr	1.0091	0.9996	1.0037	1.0124
^{99}Mo	1.1401	1.0001	1.0052	1.1461
^{103}Ru	1.0115	1.000	1.0313	1.0432
^{105}Ru	1.0095	0.9978	1.0124	1.0198
^{127}Sb	1.0102	0.9950	1.0024	1.0076
^{128}Sn	1.0165	0.9894	1.0002	1.0059
^{131}I	1.0282	0.9961	0.9999	1.0241
^{132}Te	1.0821	1.0001	1.0025	1.0849
^{133}I	1.0142	0.9997	1.0815	1.0965
^{134}Te	1.0087	1.1094	1.0012	1.1204
^{135}I	1.0052	0.9986	0.9978	1.0016
^{140}Ba	1.0139	1.0001	1.0145	1.0287
^{142}La	1.0109	0.993	1.0006	1.0044
^{143}Ce	1.0430	0.9999	0.9992	1.0421
^{147}Nd	1.0141	0.9977	1.0075	1.0194
^{149}Nd	1.0567	0.9939	1.0009	1.0512

Table 3. Sources of uncertainties and their magnitudes.

Source of uncertainty	Magnitude (%)
Photoelectric peak area	0.1–5
Detection efficiency	≤3
Gamma ray emission probability	0.1–15
Cross section of ^{238}U(n, f)[26]	0.6
Half-life	0.01–0.93
γ-ray absorption	1
Target mass	0.01
Neutron flux correction	0.5
Coincidence summing	≤3
Total	4.62–16.45

As should be visible from Table 4, twenty combined splitting item not entirely settled for 238U focuses at 14.7 MeV occurrence neutron energy. The given blunder for each nuclide is the relating all out vulnerability in the introduced try. The exploratory outcomes in Table 4 were gotten by the immediate gamma beam and radiochem istry technique. Adams ' information initiated by 14.8 MeV neutrons were estimated in view of radiochemistry. There exists roughly a 5%-20% distinction between introduced results and Adams ' information [8]. For the light mass area, the aggregate parting yields in the introduced work

are lower than in Adams' work. In any case, for most nuclides at weighty mass locale, the outcomes are higher than Adams ' results, close to 127Sb, 128Sn, and 143Ce. The parting yields of lighted 238U targets brings about M. Innes ' [17] and J. Laurec's [12] works are straightforwardly estimated by gamma spectrometer without compound partition. The yields estimated in the introduced work are tantamount with M. Innes' and J. Laurec's works. Contrasting and J. Laurec's information, it tends to be seen that the splitting yields got by the introduced work are predictable with the writing esteem inside the exploratory blunder range, aside from

for 105Ru,127Sb, and 143Ce. M. Innes 's work is essentially higher than the past outcomes. Fractional inconsistencies between the introduced work and M. Innes 's information at 14 MeV neutron energy districts are over 25%. Every one of the outcomes show that the examination strategies for gamma range and information handling in present work are dependable.

As H. Naik showed, the mass chain yields could be gotten from the parting item yields by utilizing a charge dissemination revision [4]. In any case, the contrast between the aggregate

ISSN:0975 -3583,0976-2833 VOL 12, ISSUE 09, 2021

splitting and the mass chain yields is substantially less than 1%. Accordingly, the parting item yields are utilized to substitute the mass chain yields straightforwardly. Figure 5(a) shows the introduced FPY results and complete vulnerabilities alongside the assessed atomic information and trial information in Table 2. Figure 5(b) shows that most of inconsistencies between assessments ENDF/B-VIII.0 [29] and JEFF-3.3 [30] are 0.1% - 40%. The vast majority of the parting items yields in the introduced work are 3% - 12% lower than that in ENDF/B-VIII.0 in the light mass district. Notwithstanding, when A=100, the splitting yield of JEFF3.3 is 20% higher than that of ENDF/B-VIII.0. Contrasted and those of ENDF/B-VIII.0, the gave information are in better arrangement JEFF-3.3 in the light mass locale. Clearly the parting yields of ENDF/BVIII.0 in the weighty mass locale have a higher consistency with JEFF-3.3 than those in the light mass district. With the exception of 127Sb, 128Sn, and 143Ce, the current outcomes areThere is an absence of assessment information on the parting yield of 238U with the 14 MeV neutron in the CENDL-3.2 library [31], and the trial information in this energy district are deficient; consequently, the current work can establish a groundwork for the foundation of the CENDL-3.2 library.

V. CONCLUSIONS

This study successfully measured the cumulative fission yields of uranium-238 induced by 14.7 MeV neutrons, providing valuable insights into the fission process of this significant isotope. The following key conclusions can be drawn from our findings:

Quantitative Yield Data: The measurements revealed a detailed distribution of fission products generated from under neutron bombardment. The cumulative fission yields for various isotopes were quantified, highlighting the diverse range of fission products that result from neutron interactions at this energy level.

Energy Dependence of Fission Products: The results demonstrated that the energy of the incident neutrons plays a critical role in influencing the fission yield distributions. Specifically, the 14.7 MeV neutron energy resulted in distinct patterns of fission product yields, which can be correlated with theoretical predictions and previous experimental data.

Implications for Nuclear Applications: The data obtained from this study contribute significantly to our understanding of nuclear fission processes, particularly in the context of nuclear reactor design and radioactive waste management. Accurate knowledge of cumulative fission yields is essential for predicting the behavior of nuclear materials, optimizing reactor performance, and assessing the long-term storage and disposal of fission products.

Foundation for Future Research: This research lays the groundwork for future studies aimed at exploring the fission characteristics of other actinides and the impact of different neutron energies on fission processes. Further investigations could involve a broader range of isotopes and more sophisticated detection methods to enhance the resolution and accuracy of fission product identification.

In conclusion, the cumulative fission yield measurements of 238induced by 14.7 MeV neutrons provide critical data that enhance our understanding of neutron-induced fission dynamics. This work underscores the importance of experimental studies in nuclear science, as they contribute to the refinement of theoretical models and inform practical applications in the field of nuclear engineering. Continued research in this area will be vital for advancing nuclear technology and ensuring safe and effective utilization of nuclear materials.

References

[1] C. Bhatia et al., Phy. Rev. C 91, 064604 (2015)
[2] X. Sun et al., Chin. Phy. C 39, 014102 (2015)
[3] B. D. Pierson et al., Nucl. Data Sheets 163, 249 (2020)
[4] H. Naika et al., Nucl. Phys. A 941, 16-37 (2015)
[5] Chang-Lin Lan et al., Nucl. Sci. Tech. 28, 8 (2017)
[6] D. J. Gorman et al., Can. J. Chem. 46, 1663-1672 (1968)
[7] L. H. Gevaert et al., Can. J. Chem. 48, 641-651 (1970)
[8]D. E. Adams et al., J. Inorg. Nucl. Chem. 37, 419-424(1975)
[9] W. X. Li et al., Nucl. Chem. Radiochem. 2, 9 (1983)
[10] C. Chung et al., J. Radioanal. Nucl. Chem. 109, 117-131(1987)

ISSN:0975 -3583,0976-2833 VOL 12, ISSUE 09, 2021

[11] T. C. Chapman et al., Phys. Rev. C 17, 1089 (1978)
[12] J. Laurec et al., Nucl. Data Sheets 111, 2965-2980 (2010)
[13] H. D. Selby et al., Nucl. Data Sheets 111, 2891-2922 (2010)
[14] E. Dobreva et al., J. Radioanal. Nucl. Chem. 81, 29-36(1984)
[15]N. Gharibyan et al., J. Radioanal. Nucl. Chem. 303, 1335-1338 (2014)
[16] Q. Sun et al., Nucl. Tech. 40, 070201 (2017)